Red Spectral Forms of Chlorophylls in Green Plant PSI− A Site-Selective and High-Pressure Spectroscopy Study[+]

Janne A. Ihalainen,*,† Margus Rätsep,‡ Poul Erik Jensen,§ Henrik Vibe Scheller,§ Roberta Croce,⊥,|| Roberto Bassi,⊥,¶ Jouko E. I. Korppi-Tommola,† and Arvi Freiberg‡

Department of Chemistry, P.O. Box 35, FIN-40014 University of Jyväskylä, Finland, Institute of Physics, University of Tartu, Riia 142, 51014 Tartu, Estonia, Plant Biochemistry Laboratory, Department of Plant Biology, The Royal Veterinary and Agricultural University, 40 Thorvaldensvej, DK-1871 Fredriksberg C, Copenhagen, Denmark, and Facolta di Scienze MM.FF.NN., Università di Verona, Strada Le Grazie-Cà Vignal, 37134 Verona, Italy

Received: March 27, 2003; In Final Form: June 11, 2003

One of the special spectroscopic characteristics of photosystem I (PSI) complexes is that they possess absorption and emission bands at lower energy than those of the reaction center. In this paper, the red pigment pools of PSI-200, PSI-core, and LHCI complex from *Arabidopsis thaliana* have been characterized at low temperatures by means of spectrally selective (hole-burning and fluorescence line-narrowing) and high-pressure spectroscopic techniques. It was shown that the green plant PSI-200 complex has at least three red pigment pools, from which two are located in the PSI-core and one, in the peripheral light-harvesting complex I (LHCI). All of the red pigment pools are characterized by strong electron−phonon coupling. A Huang−Rhys factor of 2.9 found for the red pigments of LHCI is the largest found for any photosynthetic antenna system. This contrasts with the bulk pigments in the main Q_y absorption band of chlorophyll *a* pigments for which the Huang−Rhys factors of less than unity are observed. This electron−phonon coupling difference of the red and bulk pigments is well reflected by the spectral dependence of the hole-burning efficiency, which is significantly reduced in the red absorption region. As a result of extremely low hole-burning efficiency in the red absorption band of LHCI, the hole-burning spectra of the PSI-200 complex mainly originate from the red pigments of the PSI-core complex. At the same time, the source of the red emission in PSI-200 is the red pigments of LHCI, in agreement with previous studies. The hole-burning spectra of PSI-core complexes from green plant and cyanobacteria are similar, both in red and bulk absorption regions. High-pressure spectroscopy data reveal dramatically larger pressure-induced linear shift rates for the redmost absorption and emission bands relative to those of bulk absorption bands. This is interpreted as due mostly to increased conformational mixing between the locally excited and charge transfer configurations of the red pigment aggregates. On the basis of analysis of available experimental data, we suggest that pigment dimers are probably responsible for the redmost states. Consequently, the excited red states can be interpreted as excimer states.

Introduction

The green plant photosystem I (PSI-200) is a large protein complex, which works as an oxido-reductant in oxygenic photosynthesis. It transports electrons from plastocyanin through a thylakoid membrane to $NADP^+$. Sunlight provides energy for this process. Light is captured by two antenna complexes of the PSI-200: the PSI-core antenna and the peripheral antenna light-harvesting complex I (LHCI).

The PSI-core complex consists of at least 14 protein subunits from which the main building block is called PSI-A/B complex. Six chlorophyll *a* (Chl *a*) molecules in the center of the complex form the reaction center.[1] The reaction center is surrounded by a core antenna that contains ∼90 Chl *a* molecules and ∼22 *β*-carotene molecules. Recently, the atomic structure of the PSI complex from cyanobacterium *Synechococcus elongatus,* has been resolved with a resolution of 2.5 Å.[2] Although cyanobacteria lack the LHCI complex, strong similarities in biochemical and spectroscopic properties suggest comparable structures of the green plant PSI-core and cyanobacterial PSI complexes.

The LHCI complex of green plant PSI consists of four different polypeptides (Lhca1−Lhca4) in a form of two or three homo/heterodimers, all located on one side of the core complex.[3,4] Each Lhca protein binds in total about 10 Chl *a* and Chl *b* molecules, with a stoichiometric ratio of about 4 to 1. In addition, the Lhca proteins also bind two or three xanthophyll molecules.[5]

In the green plant PSI-200 complex, the main Q_y absorption band of the lowest-energy singlet state of Chl *a* is located at 680 nm, and that of Chl *b* molecules, at ∼650 nm (Figure 1). A special feature of the PSI systems is the presence of red

[+] Abbreviations: PSI, photosystem I; LHCI, light-harvesting complex I; HB, hole-burning; FLN, fluorescence line-narrowing; S-factor, Huang-Rhys factor; IDF, inhomogeneous distribution function; ZPL, zero-phonon line; P700; special pair of PSI.

* Corresponding author. Fax: +31204447999. E-mail: janihal@nat.vu.nl. Present address: Department of Physics and Astronomy, Vrije Universiteit, De Boelelaan 1081, 1081 HV Amsterdam, The Netherlands.

† University of Jyväskylä.

‡ University of Tartu.

§ Royal Veterinary and Agricultural University.

⊥ Università di Verona.

|| Present address: Istituto di Biofisica, CNR sezione di Milano, via Celoria 26, 20133 Milano, Italy.

¶ Present address: Université Aix-Marseille II, LG BP-Faculté des Sciences de Luminy, Département de Biologie, Case 901-163, Avenue de Luminy, 13288 Marseille, France.

10.1021/jp034778t CCC: $25.00
Published on Web 08/02/2003

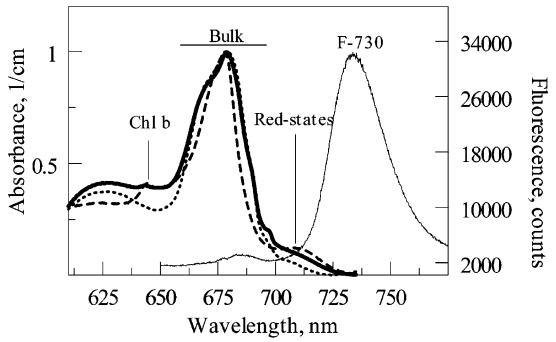

Figure 1. Q_y absorption spectra of PSI-200 (thick solid line), PSI-core (dotted line), LHCI (dashed line) at 4 K, and fluorescence emission spectrum of PSI-200 from *Arabidopsis thaliana* at 77 K.

pigments absorbing above 700 nm, the absorption maximum of the primary electron donor of the reaction center, P700. At cryogenic temperatures, red pigments work as excitation traps that lead to strong red emission bands. The emission maximums under nonselective excitation are at ∼720 nm (conventionally denoted as F-720), at ∼733 nm (F-730), or at ∼735 (F-730) for the PSI core, LHCI, and PSI-200, respectively. The redmost F-730 emission band of PSI-200 has been shown to originate from LHCI[6,7] and, more closely, from Lhca3 and Lhca4 subunits.[5,8,9]

Most of the PSI complexes (including cyanobacteria, algae, and green plants) have some red pigments, although the number of chromophores in the red pigment pools and their excitation energies vary in different species.[10,11] Several authors have attempted to locate these red pigments in the PSI core complex of *S. elongatus* by using the known structure and quantum chemical calculations.[2,12,13] The only red forming dimer, which has been pointed out in each of those studies, is the A32−B7 dimer (notification taken from Jordan et al. in ref 2), but more binding sites for red chlorophylls need to be located in order to explain the red spectral forms of *S. elongatus*.

In addition to the large red shift (∼1000 cm^{-1} from that of Chl *a* in typical organic solvents), the spectra of the red pigments show other extraordinary properties distinguishing them from the bulk antenna pigments, such as big homogeneous broadening and Stokes shift, both indicators of a strong electron−phonon coupling. A convenient technique to investigate electron−phonon coupling associated with electronic transitions in condensed phases is line-narrowing spectroscopy. In this work, both hole-burning (HB) and fluorescence line-narrowing (FLN) experiments were performed to characterize the red spectral forms of chlorophylls in green plant PSI. In past years, several spectrally selective studies on PSI particles have been carried out, separately using either FLN or HB methods.[14−16] None of these investigations applied simultaneously both techniques. Moreover, no HB studies on the red pigments of PSI particles from eukaryotes have been presented so far. A combined approach similar to ours was only recently applied for investigation of photosystem II antennae.[17,18]

In the present work, the green plant PSI-200 was studied along with its isolated PSI-core and LHCI subcomplexes in order to determine the spectral properties of the red pigments of each subcomplex of PSI-200. We show that the HB spectra of PSI-200 originate from the red pigments of the PSI-core, whereas in agreement with previous studies, the fluorescence spectra originate from the red pigments of LHCI.[7] High-pressure effects on conventional (broadband) absorption and emission bands of PSI complexes have been studied additionally. We conclude that the large pressure-induced shift rates observed are mostly related to strong interpigment couplings, as also previously assumed.

Materials and Methods

Sample Preparation and Spectroscopic Measurements. The PSI-200 samples were isolated from *Arabidopsis thaliana* thylakoids, using β-DM detergent and an ultracentrifugation technique, as described in refs 6 and 19. In the experiments, the samples were diluted in buffer containing 20 mM Bis-Tris (pH 6.5), 20 mM NaCl, and 0.06% β-DM and 60% (v/v) glycerol. The LHCI and PSI-core complexes were diluted in 10 mM Tris (pH 7.8), 0.06% β-DM, 0.1 M sucrose, and 60% (v/v) glycerol containing buffer. Monomeric Chl *a* molecules in polystyrene were prepared by mixing dissolved Chl *a* molecules in acetone and dissolved polystyrene in acetone. The mixture was cast on a Petri dish and dried for 12 h in 45 °C under vacuum. The Chl *a* molecules were prepared by the large-scale method of Hynninen.[20]

The optical density (OD) of the samples in an ∼1-cm-thick sample cell varied between 0.5 and 2.0 at 680 nm, depending on the experiment. In most concentrated preparations, the OD was below 0.2 at 710 nm, still suitable for the red wing excited fluorescence experiments. The thickness of the Chl *a* in polystyrene was ∼2 mm with OD of 0.1. For the fluorescence and hole-burning measurements, the samples were cooled to 4.2 K in a liquid helium cryostat (Utreks, Ukraine). No reductants were used in the experiments.

A Ti/sapphire CW solid-state laser (model 3900S, Spectra Physics) with line width of 0.07 cm^{-1} and a dye laser (model 375, Spectra Physics) with line width of 1−2 cm^{-1} were used for the red band and ∼680 nm excitation, respectively. Both lasers were pumped by an Ar^+ ion laser (model 171, Spectra Physics). In most cases, the burning power was set to 10 mW, and the illuminated area on the sample was ∼1 cm^2. Burning times were adjusted between 30 s and 4 min for proper holes without saturating the sample. For the transmission measurements, a 12-V tungsten lamp was used. Detection was performed by using a 0.6-m monochromator (MDR-23, LOMO, Russia) and an electrically cooled CCD camera (Andor Technology). Spectral resolution varied between 0.1 and 0.4 nm, depending on the grating used. The emission spectra were corrected to the spectral sensitivity of the apparatus.

The high-pressure system used is analogous to the one described earlier in ref 21. Briefly, it consists of a three-stage gas compressor, a high-pressure cell (both Unipress, Poland), and a unique homemade bubble-free liquid nitrogen cryostat. In this system, helium gas is exploited as the pressure-transmitting medium. The high-pressure cell has two optical plugs with sapphire windows located at opposite sides of the cylindrical cell body. The sample, prepared as described above, in a gelatin capsule of ∼0.3 mL volume was placed in the center of the high-pressure cell. The helium gas pressure inside the cell was measured with better than ±0.1 kbar accuracy using a manganin resistance gauge situated inside the third stage of the compressor. The temperature was determined with a Si diode attached to the outside of the massive cell body. Since proteins need some time to reach an equilibrium at fixed pressure, measurements at each pressure were carried out after a 5−10-min waiting period. To ensure measurements of elastic (reversible) pressure effects, the spectra were detected when going up and coming down with pressure.

Simulations of HB and FLN Spectra. The measured HB and FLN spectra have been analyzed using the model introduced

by Hayes et al.[22,23] In this model, developed for localized excitations, a low-temperature limit is assumed, and the coupling is restricted to a distribution of protein phonons. No high-frequency intramolecular vibrations are taken into account. As introduced in ref 23, the one-phonon sideband can be assumed to have a two-peak shape with various frequencies. All distributions are taken of Gaussian form, with the mean frequency ν_{mk} and the width Γ_k. Here and below, the width means full width at half-maximum. A single-site absorption (or emission) spectrum can then be expressed as

$$L(\nu - \Omega) = e^{-S_T} \prod_{k=1,2} \sum_{R=0}^{\infty} \frac{S_k^R}{R!} l_{R,k}(\nu - \Omega \mp R\nu_{mk}) \quad (1)$$

Here, S_T is the total ($S_1 + S_2$) and S_k the kth phonon Huang−Rhys factor characterizing the linear electron−phonon coupling strength, R is the number of phonons coupled to the electronic transition, $l_{R,k}$ is the line shape function. At $R = 0$, eq 1 describes the zero phonon line (ZPL) centered at frequency Ω. Equation 1 distinguishes an absorption spectrum when summation is over negative $R\nu_m$ terms and an emission spectrum, otherwise.[17] The line shape function, $l_{R,k}$, with $R \geq 1$ gives the phonon profile. The conventional nonselective absorption (emission) spectrum can be obtained by convoluting the properly normalized single-site absorption (emission) spectrum with the inhomogeneous distribution function (IDF) mimicking inhomogeneous broadening of the spectra. A Gaussian-shape IDF, $N(\Omega\text{-}\nu_c)$, is generally assumed with the mean frequency ν_c and width Δ.

The absorption (emission) spectrum after a narrow-band burning (excitation) at laser frequency ν_B during time τ is given by

$$A_\tau(\nu) = \int d\Omega\, N(\Omega - \nu_c) e^{-\sigma I \Phi \tau L(\nu_B - \Omega)} L(\nu - \Omega) \quad (2)$$

Here, $N(\Omega - \nu_c)$ together with the exponential term represents the modified IDF centered at ν_c. σ, I, and Φ are the absorption cross-section, laser intensity, and quantum yield of phototransformations, respectively. Equation 2 at $\tau = 0$ describes the nonselectively excited absorption (emission) spectrum. The site-selective spectra for $\tau \neq 0$ can be obtained by taking the difference $A_\tau - A_0$.

Results and Discussion

Figure 1 presents an overview of the Q_y absorption spectra of all the complexes studied as well as of the nonresonantly excited fluorescence emission spectrum of the PSI-200 complex at low temperatures. In all samples, clear absorption bands between 700 and 720 nm can be observed. On the basis of the chlorophyll content of each protein complex, it was concluded in ref 10 that the LHCI complex has relatively stronger red absorption than the PSI-core complex. The red absorption maximums were determined around 708 nm for the PSI-core complex and around 712 nm for both the LHCI and PSI-200 complexes. The emission band of the PSI-200 complex at ~734 nm originates from the red pigments of the LHCI complex, and the small band around 685 nm, from the "bulk" pigments, which are unable to transfer energy either to the reaction center or to the red pigments.

Effects of the Nonresonant HB. Several different pigment pools with characteristic transition energies are contributing to the Q_y absorption spectrum of the complexes shown in Figure 1.[10] Assuming that at low temperatures these pools are connected by downhill energy transfer, the spectral position and the width of the IDF of the pools could be identified by exciting with a narrow-band laser into the bulk absorption band and detecting the resulting broad (nonresonant) HB spectra.

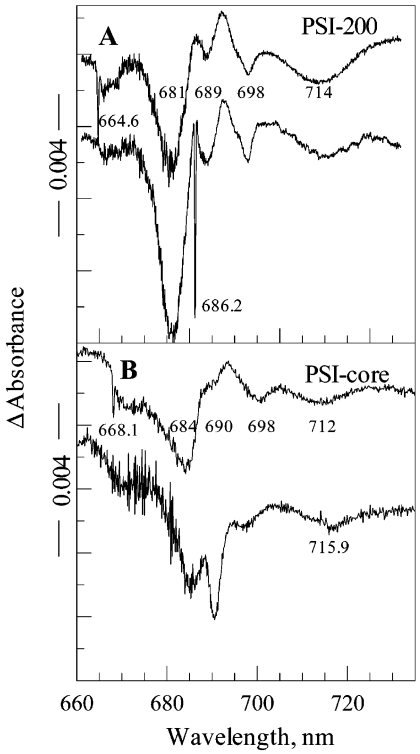

Figure 2. Nonresonant HB spectra of PSI-200 (A) and PSI-core (B) at 4.2 K. The excitation wavelengths (664.6 and 686.2 nm for PSI-200; 668.1 and 715.9 nm for PSI-core) are noted in figures. The spectra measured using two different burning wavelengths (denoted by resonant narrow ZPL holes) are vertically shifted relative to each other for clarity. The main broad satellite holes are indicated. The burning fluences were ~6 J/cm^2 for PSI-200 and ~12 J/cm^2 for PSI-core.

As seen in Figure 2, a series of broad satellite holes of the narrow ZPL hole, which appears at the excitation wavelength, have been observed in PSI-200 and PSI-core complexes after burning at the blue side of the bulk absorption band (at 665−668 nm) or at its red side. General features of the spectra (in terms of the number of bands and their position) obtained for each sample using different excitation wavelengths are similar. This indicates that the final states probed under the present experimental conditions are the same. The most prominent satellite bands for the PSI-200 (PSI-core) complex are located at 681 (684), 689 (690), 698 (698), and 714 (712) nm. The 690 nm band is relatively very weak in the PSI-core upon blue side excitation.

It is notable that the 681 (684) nm band, together with the whole satellite band pattern, appears also when burning at longer wavelengths. As a result of energy conservation, this band cannot represent the pool of weakly coupled pigments populated via energy transfer. One possibility is that it belongs to the higher exciton states of a pool of strongly coupled pigments, either in the core antenna or in the reaction center, whose lowest energy states get populated via downhill energy transfer. Another interpretation, based on mild structural reorganizations accompanying energy transfer, was suggested in ref 15. The exciton version gets strong support by burning at the red most absorption band of PSI-core (see Figure 2B), which results in structured bleaching in the 665−700-nm spectral region similar to that seen at short-wavelength burning. The differences in the intensity pattern of the spectra are most probably caused by the interplay of holes with photoproduct-formed antiholes that vary with burn wavelength and are characteristic of the HB

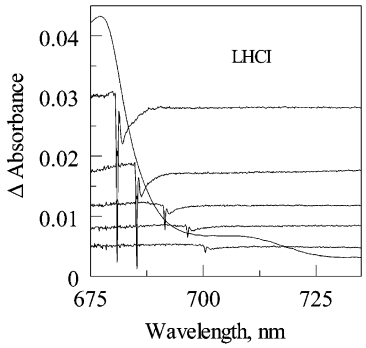

Figure 3. Hole-burning spectra of LHCI. The burning fluency was ~ 12 J/cm^2. The dotted curve in the background is the absorption spectrum. The hole spectra are magnified 20 times and shifted with respect to each other along the vertical axes.

technique. It is worth noticing a similar 665−700-nm structure of the red-excited HB spectrum of PSI-core and that of the transient photobleaching spectrum of PSI particles from green algae *Chlamydomonas reinhardtii*, also measured at low temperatures (Gibasiewicz, personal communication).[24] In the latter case, the spectral peaks were assigned to collective excitations of the reaction center pigments, along with the two connecting chlorophylls (See ref 2).

A comparison HB spectral pattern reveals that the nonresonant HB spectra of PSI complexes from green plants and cyanobacteria are almost identical, which can be considered as an indication of the structural similarity of their core complexes.[15,16] An important observation is that, apart from about 2-nm red shift, the redmost satellite hole band of the green plant PSI-200 is located at the same position as in PSI complexes of cyanobacteria.[11,15,16] A similar small red shift of the redmost satellite hole band in PSI-200 relative to that in the PSI-core can also be seen in Figure 2A and B. It is, therefore, reasonable to assign the redmost satellite band observed in PSI-200 to the red pigments of the PSI-core assembled into the PSI-200 complex.

Although the nonresonant HB spectra of PSI-200 and PSI-core are fairly similar to each other, they both drastically differ from the spectra for the LHCI complex shown in Figure 3. As seen in this figure, the ZPL holes, located at the burning wavelengths, are accompanied from the lower energy side by well-developed pseudophonon sideband (PSB) holes. The real sideband hole from the higher energy side is not resolved, presumably because of overlap with the product-formed antihole. No broad satellite holes have been observed in the LHCI complex. The ZPL hole depth gradually decreases toward larger excitation wavelengths, roughly following the shape of the bulk absorption spectrum. From the total area under the PSB hole and the ZPL hole relative to that of the ZPL hole alone, the upper limit of the linear electron−phonon coupling factor, *S*, can be estimated. In the present case, *S* is between 0.6 and 0.8, corresponding to moderate coupling strength.

The lack of the broad satellite hole at ~714 nm in the LHCI complex is surprising, because it possesses the strongest red absorption among all studied complexes (see Figure 1). Moreover, the red spectral forms of LHCI are assumed to be responsible for most of the fluorescence emitted by the PSI-200 complex at low temperatures.[6,7] We stress that the nonselectively excited fluorescence spectrum of our LHCI sample (not shown) is both similar to the F-730 emission band of PSI-200 in Figure 1 and also indistinguishable from the previously reported LHCI fluorescence spectra. This proves that the majority of the red pigments in our LHCI sample are in native conformation. We can provide two explanations for this puzzle here: (i) the red pigments have extremely low burning efficiency and (ii) the pigments accepting excitation in the present experiment are not coupled to the red pigments. The data shown below clearly support the former option. The burning efficiency is closely related to phonon coupling strength, and the red pigments of LHCI have very strong phonon coupling (high *S* factor, Table 2) which leads to low burning efficiency. Indeed, even direct excitation into the absorption band of red pigments produces only very shallow holes (see the redmost curve in Figure 3 as well as Figure 5C and Table 1).

TABLE 1: Burning Efficiency of PSI Complexes in the Red Absorption Band Region[a]

burning wavelength (nm)[b]	PSI-200	PSI-core	LHCI
695	1.3	3.2	0.2
700	0.9	2.9	0.1
705	0.4	1.0	<0.1
710	0.4	1.0	<0.1
715	0.3	0.7	<0.1
720	0.2	0.4	

[a] The efficiency presented in % units was determined as a depth of the ZPL holes in HB spectra relative to the optical density of the sample at the burning wavelength. [b] Experimental uncertainty, ± 1 nm.

TABLE 2: Simulation Parameters for the Lowest-Energy Red Antenna States of PSI Complexes[a]

	PSI-200		PSI-core		LHCI
parameters[b]	FLN	HB	FLN	HB	FLN
S_1	2.8	1.6	0.4	1.6	2.7
S_2	0.2	0.6	1.9	0.6	0.2
ν_{m1} (cm^{-1})	100	21	21	21	110
ν_{m2} (cm^{-1})	170	92	92	92	190
Γ_1 (cm^{-1})	130	12	12	12	141
Γ_2 (cm^{-1})	88	104	104	104	88
γ (cm^{-1})[c]	1.5	1.5	1.5	1.5	1.5
λ_C (nm)	721	716	715	716	720
Δ (cm^{-1})	389	294	377	294	359
E_{em}[d] (nm)	733/734	718/−	722/722.5	718/−	732/732
E_{abs}[d] (nm)	710/711	714/714	706/708	714/714	709/711

[a] FLN and HB stand for the fluorescence line-narrowing and hole-burning spectra, respectively. *S* is the Huang−Rhys factor, γ is the ZPL width, ν_{Mi} and Γ_i are the mean frequencies and widths of phonon distributions, respectively, and λ_C and Δ are the position and width of IDF. The last two rows indicate the calculated (according to eq 2 with $\tau = 0$) and experimental maximums of broadband absorption and emission spectra. [b] Relative standard deviation of the parameters is ±10%, except for λ_C, E_{em} and E_{abs}, for which the uncertainty is ±2 nm. [c] Experimentally limited value. [d] Indicated is the simulated value versus the experimental value.

Line-Narrowing Spectroscopy of the Redmost Antenna States. Figure 4 demonstrates the fluorescence spectra of PSI-200, PSI-core, and LHCI complexes excited with a narrow-band laser directly into the red spectral forms. As can be seen, despite resonant excitation, the fluorescence spectra of all samples are broad and structureless. Similar spectra were reported earlier for PSI-200 by Gobets et al.[14] and for LHCI by Ihalainen et al.[7] Apart from a linear shift of emission maximums characteristic of inhomogeneously broadened spectra,[14] there is very little change of fluorescence band shapes with excitation wavelength.

Hole-burning spectra of PSI-200, PSI-core, and LHCI complexes at red-band excitation are shown in Figure 5. The spectra of PSI-200 (Figure 5A) are similar to those of cyanobacterial PSI complexes reported by Small and co-workers.[15,16] So is the spectrum of the PSI-core complex in Figure 5B, at least at its low-frequency region close to the ZPL hole. With the plant PSI-core complexes, a proper spectral baseline was not obtained,

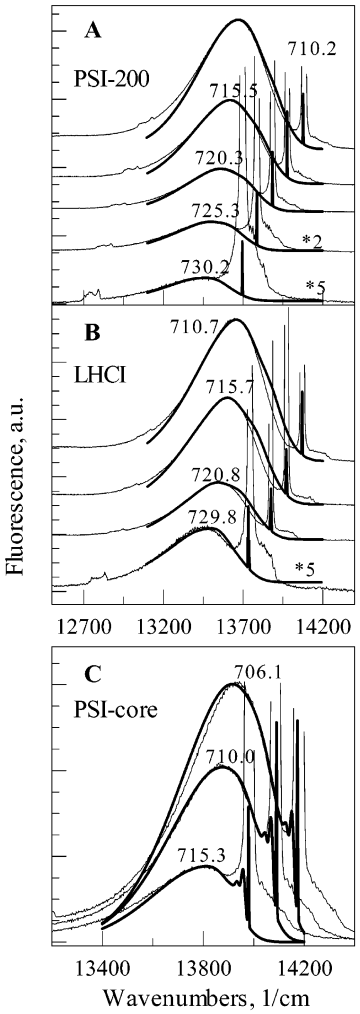

Figure 4. Experimental fluorescence spectra after narrow-band laser excitation (thin lines) of PSI-200 (A), LHCI (B), and PSI-core (C), together with simulated curves (thick lines). The simulation parameters are shown in Table 2. The measured spectra are corrected for the spectral sensitivity of the detection apparatus. The large spikes at excitation wavelengths (indicated in figures in nanometers) are scattering artifacts. The red most excited spectra (730.2 nm for PSI-200 and 729.8 nm for LHCI) are multiplied by 5.

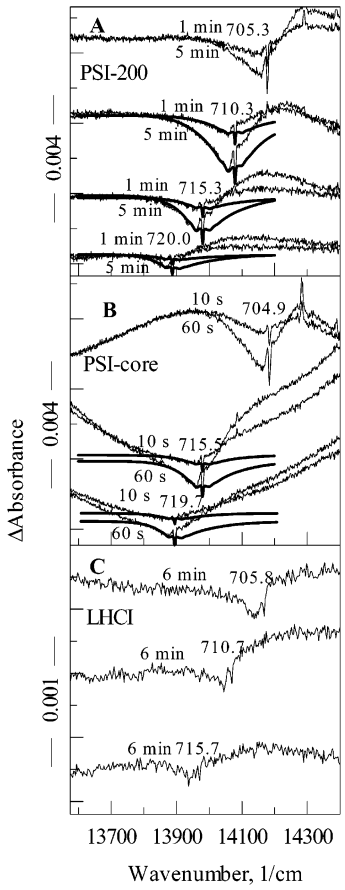

Figure 5. Hole-burning spectra (thin lines) of PSI-200 (A), PSI-core (B), and LHCI (C) upon red pigment excitation, along with the simulated spectra shown with thick continuous curves. The excitation wavelengths (in nanometers) and burning times are indicated. The excitation power density was ~10 mW/cm^2 in each experiment. The simulation parameters are shown in Table 2.

although the burning efficiency was rather high (see Table 1). It is likely that once the peripheral LHCI complex is separated from PSI-200, the stability of the remaining core complex decreases, allowing for larger structural reorganizations under illumination, which are difficult to control. As long as illumination induces an absorption increase from the low-energy side of the redmost absorption band, formation of charged chlorophylls, in addition to the $P700^+$ state absorbing around 820 nm,[25] is probable. We also failed to obtain high-quality spectra for the LHCI complex (Figure 5C), this time as a result of low HB efficiency, as already discussed. According to Table 1, the HB efficiency for LHCI is more than an order of magnitude less than for PSI-core. A smaller burning efficiency of PSI-200 compared with that of PSI-core and similarity of their HB spectra implies that the holes burned into the PSI-200 complex originate from the pigments of the PSI-core complex. One can evaluate from the burning efficiencies for different complexes that almost 40% of the redmost absorption band intensity in the PSI-200 complex is due to the PSI-core complex.

Both resonant HB and FLN spectra were simulated as described in the Materials and Methods section. The fitted spectra are shown in Figures 4 and 5 with thick solid curves, while the simulation parameters are presented in Table 2. As a matter of fact, because of baseline problems mentioned above, the HB parameters obtained from fitting of the PSI-200 spectra were directly applied for the PSI-core with reasonably good results (see Figure 5B). The last rows of Table 2 refer to the nonselective broadband absorption and emission spectra.

By analyzing the data of PSI-200, it becomes immediately clear that the simulation parameters obtained from the HB spectra are similar to those of the PSI-core, whereas the parameters deduced from the FLN spectra are similar to those of LHCI. This is in line with the idea that the resonant HB spectra of PSI-200 originate from the red pigments of PSI-core and that its fluorescence is due to the red pigments of the LHCI complex. The IDF widths, 359 and 389 cm^{-1}, obtained for PSI-200 and LHCI, respectively, agree very well with earlier studies.[7,14] The total S factor for both LHCI and PSI-200 fluorescence has been determined to be ~3, and the phonon frequencies turned out to be rather high (values of 100 and 170 cm^{-1}). To the best of our knowledge, the phonon coupling terms represent the strongest coupling found among all photosynthetic antenna complexes, which naturally leads to large lattice relaxation energy and, therefore, to a strong Stokes shift. Still higher S factors have only been observed for the reaction centers of purple bacteria.[26]

The HB parameters obtained in this work agree with the data for the PSI-core complexes from cyanobacteria (Table 3).[16,23] It also appears from Table 2 that in the case of the PSI-core complex, a rather different set of parameters was needed for

TABLE 3: Comparison of the HB Simulation Parameters of the Red Pigments for the Green Plant[a] and Cyanobacterial PSI-Core Complexes

parameter	PSI-core, this work	PSI-core[b]	PSI-core[c]
S_1	1.6	1.8	1.6
S_2	0.6	0.4	0.4
ν_{m1} (cm^{-1})	21	20	18
ν_{m2} (cm^{-1})	92	110	70
Γ_1 (cm^{-1})	12	14	15
Γ_2 (cm^{-1})	104	100	65
γ (cm^{-1})	1.5[d]	0.5	0.5
ν_c (cm^{-1})	13986	13822	13947
Δ (cm^{-1})	294	250	300

[a] *Arabidopsis thaliana*, this work. [b] *Synechococcus elongatus*.[11] [c] *Synechocystis PCC6803*.[16] [d] Experimentally limited value.

absorption (HB) and emission simulations. In absorption, the lower-frequency vibrations seem to be more strongly coupled to the electronic transition than the higher-frequency ones, whereas in emission, only the higher-frequency vibrations are observed. It was realized previously in several photosynthetic complexes that the low-frequency modes could easily be observed in HB, but rarely in FLN spectra where mostly higher frequency modes dominate (see, e.g., Pullerits et al.[27] for the case of the B820 complex from purple photosynthetic bacteria). This situation is well characterized in the present work by the LHCI data. Although the holes in Figure 5C are so shallow that simulations turned out to be meaningless, the low-frequency modes are clearly present. In contrast, in fluorescence (Figure 4C), only high-frequency modes can be seen. One explanation provided is entirely technical, that the strong scattering due to the exciting laser masks the low-frequency structure of the emission spectrum. Although viable, this is obviously not always the case, as shown for the PSI-complex of *Synechocystis* PCC 6803.[10] In addition, in the case of FLN spectra of the PSI-core complex in Figure 4C, the low-frequency modes may be present.

Using the two different parameter sets obtained for PSI-core from separate fittings of FLN and HB spectra, the corresponding nonselective emission and absorption spectra were simulated. Mirror symmetry between conjugated absorption and emission spectra was assumed, generally well-founded for chlorophyll-like molecules. Deviations from this rule in the case of localized states are possible only if the corresponding pairs of potential energy surfaces mediating absorption and emission transitions are different.[28,29] The calculated band positions are listed in the last two rows of Table 2, together with the experimentally determined values. Simulations with PSI-core FLN data yield the emission maximum at 722 nm and the absorption maximum at 706 nm, which are close to experimentally observed values 722.5 and ~708 nm, respectively. By using the HB data, the simulated absorption spectrum lies at 714 nm, which is close to the 712-nm band resolved by nonresonant hole burning (Figure 2B). The corresponding emission spectrum should locate at 718 nm. This component is not observed experimentally; it might be obscured by a more intense 722.5-nm fluorescence band. These simulations suggest that there are two types of red pigments in the PSI-core giving rise to absorptions around 706 and 714 nm. The 706-nm pigments are characterized by a total Huang−Rhys factor of $S = 2.3$ and a large lattice relaxation energy. Their IDF locating at 715 nm has a width of 377 cm^{-1}. For the 714-nm pigments, $S = 2.2$, and the IDF lies at 716 nm and has a width of 294 cm^{-1}.

To further demonstrate the essential differences between the two sets of red pigments in PSI-core, the experimental FLN spectra of the complex are compared in Figure 6A with the simulated spectra using the parameters, which have been

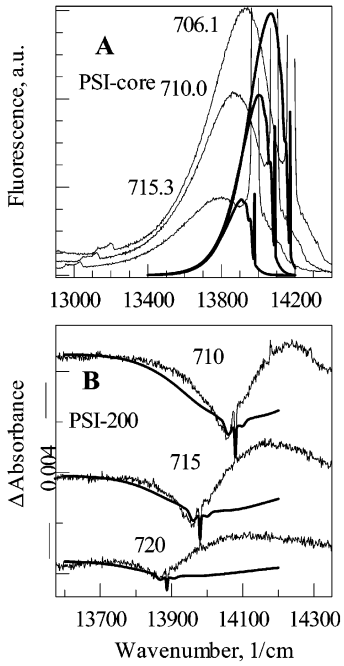

Figure 6. (A) Experimental fluorescence spectra at spectrally selective excitation of the PSI-core complex (thin curves) along with the simulated spectra (thick curves) using the parameters obtained from the fitting of the HB spectra shown in Figure 4. See more details in the text. (B) Experimental HB spectra of PSI-200 (thin curves) together with the simulated spectra (thick curves) using the parameters obtained from the fitting of the FLN spectra of the PSI-core complexes (see Table 2)

obtained from the fitting of the HB spectra of the same complex. Analogous comparison relative to experimental HB spectra is given in Figure 6B. Here, the simulation parameters used are those obtained from the fitting of the PSI-core emission, whereas the experimental spectrum is of the PSI-200 complex instead of the PSI-core, as a result of the baseline problem in the latter complex (see above). As seen, the simulated FLN spectra fail in describing the high-frequency part of the experimental spectra, while the situation is more or less opposite in the case of HB spectra. In the latter case, the low-frequency part of the simulated spectrum is relatively too weak, but the high-frequency part seems somewhat exaggerated. We admit, as a word of warning, that according to our experience, simulations of the HB spectrum appear to be generally relatively insensitive with respect to high-frequency components of the spectrum. However, in the case of LHCII, both site-selective emission and absorption spectra could be simulated with a similar set of parameters.[18]

Pressure Dependence of Broadband Emission and Absorption Spectra. The conventional (broadband) absorption and emission spectra of all three PSI complexes were studied under high hydrostatic pressure at 80 K to get more insight into the pigment−pigment and electron−phonon coupling effects. Monomer Chl *a* molecules imbedded into a polymer matrix (mimicking the protein surroundings) was used as a reference system in these measurements.

Figure 7 depicts the data concerning the pressure-induced shift of the redmost band maximums in PSI complexes. They all demonstrate a linear red shift with increasing pressure. At the same time, the bandwidths remain unchanged within the experimental uncertainty. The shift rates obtained are gathered in Table 4. As expected, the F-730 fluorescence band shift rate is fairly similar in PSI-200 (−50.4 cm^{-1}/kbar) and in LHCI (−54.1 cm^{-1}/kbar). This once again points to their common origin. A slightly larger shift found for LHCI may be due to its

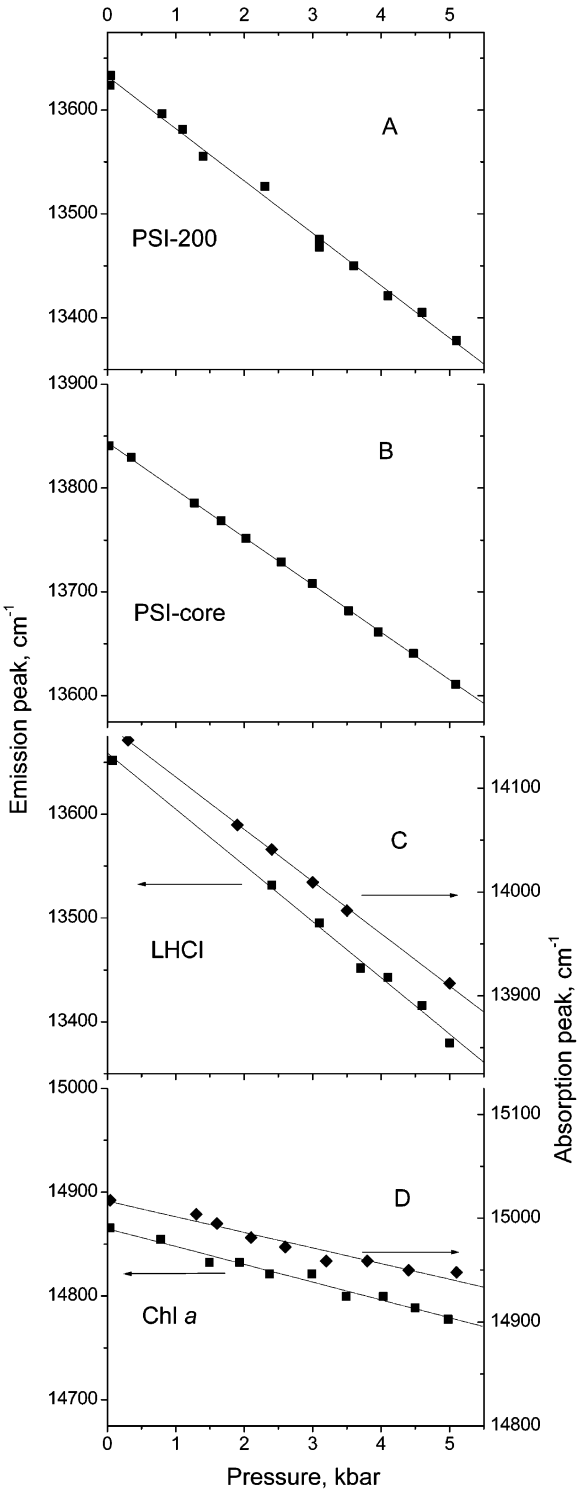

Figure 7. Pressure dependence of the nonselectively excited fluorescence/absorption maximums of PSI-200 (A), PSI-core (B), LHCI (C), and monomeric Chl *a* embedded in polymer (D) at 77 K. The linear regression lines yield the following shift rates (in cm^{-1}/kbar): −50.4 for the PSI-200 fluorescence, −45.3 for the PSI-core fluorescence, −54.1 and −50.3 for the LHCI, and −16.5 and 15.1 fluorescence and absorbance, respectively (in the last two cases).

higher compressibility, as compared to the more intact PSI-200 complex. The shift rate of the F-720 band in PSI-core is also high, −45.3 cm^{-1}/kbar. The absorption counterpart of the F-730/F720 emission, the redmost absorption band, is more difficult to study because of its low intensity and large width (Figure 1). Only in LHCI does the red absorption band stand out sufficiently from the background to be reliably measured under pressure. Considering experimental difficulties, the obtained shift rate (−50.4 cm^{-1}/kbar) is almost the same as that for the emission band, suggesting that they belong to the same pair of potential energy surfaces. The pressure shift rate is also available for the HB data measured on the PSI complex of cyanobacteria,[15,16] which can be compared with the PSI-core fluorescence shift. The rates (−43 and −45.3 cm^{-1}, respectively) are again very similar. However, considering the above discussion suggesting the existence of two types of red pigments in PSI-core, this coincidence has to be regarded as accidental, differently from the case of LHCI.

TABLE 4: Linear Pressure-Induced Shift Rates Measured in cm^{-1}/kbar for the Conjugate Absorption and Emission Bands of PSI Complexes at 77 K[a]

PSI-200		PSI-core		LHCI	
absorption	emission	absorption	emission	absorption	emission
−	−50.4	−	−45.3	−50.4	−54.1

[a] The experimental uncertainty is ± 7%.

The high shift rates found for the redmost pigment systems contrast with a shift rate of the bulk absorption band that is almost an order of magnitude smaller. For instance, in LHCI, this number is −5.2 cm^{-1}/kbar (data not shown). The Chl *a* reference system shown in Figure 7D also demonstrates relatively small shift rates (−15 to −16 cm^{-1}/kbar for absorption and emission bands, respectively). Different shift rates of monomer chlorophylls in various matrixes are most likely due to different compressibility of the surroundings.

A significant parallel can be drawn with the above records and the data obtained for the LH2 antenna complex from purple photosynthetic bacteria. In the so-called B850 aggregate, in which the interpigment couplings are known to be strong (≥300 cm^{-1})[30−32] and optical excitation leads to exciton formation, the pressure shift rate of the absorption band at 80 K is high, about −40 cm^{-1}/kbar.[21] In another pigment system, B800, the interpigment couplings are thought to be so weak that excitations are localized on single bacteriochlorophyll *a* molecules, and the shift rate is only about −10 cm^{-1}/kbar.[32]

By analogy, it is reasonable to assume that the red pigments distinguish from the bulk pigments of PSI complexes first of all by strong coupling between each other. This idea corroborates with suggestions based on structural data showing that two or three strongly coupled pigments form the red states of PSI.[12−14] Further evaluation of the nature of the red excited states is possible on the basis of electroabsorption (Stark spectroscopy) measurements,[15,16,33] which reveal a charge transfer character of these states. The polar electronic states interact strongly with their surroundings, providing natural explanation to the major electron−phonon coupling observations of this and previous works. Moreover, as long as significant charge transfer is feasible only between the nearest neighbor pigments, the Stark spectroscopy data support a pairing of the pigments responsible for the red states. The excited dimers are called excimers (see ref 34 for a review). Broad emission and absorption bands with considerable Stokes shift between them characterize excimers. We thus suggest that the red bands of PSI complexes belong to an excimer. It is worth mentioning that the Stokes shift in LHCII complexes, a prototype weak electron−phonon coupling chlorophyll-protein system, is only ∼11 cm^{-1},[17] that is, much smaller than in any of the PSI red pigment pools (see Table 2).

Recent analysis of pressure-induced spectral shifts of small-radius self-trapped excitons in the B850 aggregate of LH2 revealed a contribution into the fluorescence red shift related to increased exciton−phonon coupling under compression.[21] A

change of exciton−phonon coupling under pressure can most easily be checked by observing the spectral (absorption or fluorescence) bandwidths. The latter is proportional to $\sqrt{\varpi E_{LR}}$, where ϖ is an effective vibrational frequency strongly coupled to the electronic transition, and E_{LR} stands for the lattice relaxation energy. Pressure dependence of ϖ is usually weak. Therefore, and because the bandwidths of PSI complexes are independent of pressure, it is safe to assume that E_{LR} does not noticeably change with pressure. This allows us to conclude that the large pressure-induced shift rates observed are mostly due to increased conformational mixing between the locally excited and charge-transfer configuration, leading to excimer formation.

Summary

One of the special spectroscopic characteristics of the PSI complexes is that the absorption and emission bands are at lower energy than those of the reaction center. In this study, we have characterized the red pigment pools of the green plant PSI complexes (PSI-200, PSI-core, and LHCI) using spectrally selective and high-pressure spectroscopic techniques at low temperatures. The experimental data were analyzed by means of an impurity center (localized excitation) model developed in refs 22 and 23. The key findings of the present work are as follows:

(i) Nonresonant HB spectra contain broad long-wavelength satellite holes that remain at the same position regardless of excitation wavelength. Others have found similar holes for PSI complexes of cyanobacteria, which suggests similar structures of the PSI-core complex from green plants and the PSI complex from cyanobacteria.

(ii) No long-wavelength satellite holes have been found in LHCI antenna complexes. Large electron−phonon coupling causes this very low HB efficiency. The Huang−Rhys factor for the LHCI complex is the largest found for any other photosynthetic antenna system.

(iii) Because of extremely low HB efficiency in the red absorption band of LHCI, the HB spectra of PSI-200 complexes mainly originate from the red pigments of the PSI-core complex. At the same time, the source of the emission of the PSI-200 is red pigments of LHCI, in agreement with previous studies.[6,7]

(iv) High-pressure spectroscopy data reveal dramatically larger pressure-induced linear shift rates for the redmost absorption and emission bands relative to those of bulk absorption bands. This is interpreted as due mostly to increased conformational mixing between the locally excited and charge-transfer configurations of the red pigment dimers/aggregates.

The FLN spectrum of the PSI-core complex cannot be satisfactorily fitted with the HB parameters and vice versa. The situation is cardinally different in LHCII, for which a similar set of parameters describes both site-selective emission and absorption spectra.[17] The simulations of FLN and HB spectra on PSI-core suggest that two types of red pigments are involved. The pigments absorbing at 706 nm are responsible for FLN spectra, whereas the pigments absorbing at 714 nm are related to HB spectra. Because the origins of both types of red pigments locate very closely, around 715−716 nm, experimental distinction between them is not straightforward.

Analysis of the available experimental data shows that pigment dimers are probably responsible for the red states. Consequently, the red excited states can be interpreted as excimer states. Excimer interaction is attributed to configurational mixing of neutral exciton and polar charge transfer states. This provides natural explanation to the strong electron−phonon coupling in PSI complexes observed.

Acknowledgment. The authors thank Mr. Juha Linnanto for valuable discussions and Dr. Delmar S. Larsen for careful reading of the manuscript. The EC Center of Excellence Program "EstoMaterials", the Hasselblad Foundation, and the Estonian Science Foundation Grant no. 5543 are acknowledged for financial support. The University of Jyväskylä is acknowledged for a scholarship for J.A.I.

References and Notes

(1) Scheller, H. V.; Jensen, P. E.; Haldrup, A.; Lunde, C.; Knoetzel, J. *Biochim. Biophys. Acta* **2001**, *1507*, 41−60.

(2) Jordan, P.; Fromme, P.; Witt, H. T.; Klukas, O.; Saenger, W.; Krauss, N. *Nature* **2001**, *411*, 909−917.

(3) Boekema, E. J.; Jensen, P. E.; Schlodder, E.; van Breemen, J. F. L.; van Roon, H.; Scheller, H. V.; Dekker, J. P. *Biochemistry* **2001**, *40*, 1029−1036.

(4) Jansson, S. *Biochim. Biophys. Acta* **1994**, *1184*, 1−19.

(5) Croce, R.; Morisonotto, T.; Castelletti, S.; Breton, J.; Bassi, R. *Biochim. Biophys. Acta* **2002**, *1556*, 29−40.

(6) Croce, R.; Zucchelli, G.; Garlaschi, F. M.; Jennings, R. C. *Biochemistry* **1998**, *37*, 17355−17360.

(7) Ihalainen, J. A.; Gobets, B.; Sznee, K.; Brazzoli, M.; Croce, R.; Bassi, R.; van Grondelle, R.; Korppi-Tommola, J. E. I.; Dekker, J. P. *Biochemistry* **2000**, *39*, 8625−8631.

(8) Schmid, V. H. R.; Cammarata, K. V.; Bruns, B. U.; Schmidt, G. W. *Proc. Nat. Acad. Sci. U.S.A.* **1997**, *94*, 7667−7672.

(9) Castelletti, S.; Morisonotto, T.; Robert, B.; Caffari, S.; Bassi, R.; Croce, R. *Biochemistry* **2003**, *42*, 4226−4234.

(10) Gobets, B.; van Grondelle, R. *Biochim. Biophys. Acta* **2001**, *1507*, 80−99.

(11) Melkozernov, A. N. *Photosynth. Res.* **2001**, *70*, 129−153.

(12) Byrdin, M.; Jordan, P.; Krauss, N.; Fromme, P.; Stehlik, D.; Schlodder, E. *Biophys. J.* **2002**, *83*, 433−457.

(13) Damjanovic, A.; Vaswani, H. M.; Fromme, P.; Fleming, G. R. *J. Phys. Chem. B* **2002**, *106*, 10251−10262.

(14) Gobets, B.; van Amerongen, H.; Monshouwer, R.; Kruip, J.; Rögner, M.; van Grondelle, R.; Dekker, J. P. *Biochim. Biophys. Acta* **1994**, *1188*, 75−85.

(15) Rätsep, M.; Johnson, T. W.; Chitnis, P. R.; Small, G. J. *J. Phys. Chem. B* **2000**, *104*, 836−847.

(16) Zazubovich, V.; Matsuzaki, S.; Johnson, T. W.; Hayes, J. M.; Chitnis, P. R.; Small, G. J. *Chem. Phys.* **2002**, *275*, 47−59.

(17) Pieper, J.; Schödel, R.; Irrgang, K.-D.; Voigt, J.; Renger, G. *J. Phys. Chem. B* **2001**, *105*, 7115−7124.

(18) Pieper, J.; Schödel, R.; Irrgang, K.-D.; Voigt, J.; Renger, G.; Small, G. J. *Chem. Phys. Lett*. **1999**, *310*, 296−302.

(19) Jensen, P. E.; Gilpin, M.; Knoetzel, J.; Scheller, H. V. *J. Biol. Chem.* **2000**, *275*, 24701−24708.

(20) Hynninen, P. H. *Acta Chem. Scand.* **1977**, *31*, 829−835.

(21) Timpmann, K.; Ellervee, A.; Kuznetsov, A.; Laisaar, A.; Trinkunas, G.; Freiberg, A. *J. Lumin.* **2002**, *102*, 220−225.

(22) Hayes, J. M.; Gillie, J. K.; Tang, D.; Small, G. *Biochim. Biophys. Acta* **1988**, *932*, 287−305.

(23) Hayes, J. M.; Matsuzaki, S.: Rätsep, M.; Small, G. J. *J. Phys. Chem. B* **2000**, *104*, 5625−5633.

(24) Gibasiewicz, K.; Ramesh, V. M.; Lin, S.; Woodbury, N. W.; Webber, A. N. *J. Phys. Chem. B.* **2002**, *106*, 6322−6330.

(25) Schreiber, U.; Klughammer, C.; Neubauer, C. *Z. Naturforsch.* **1988**, *43*, 686−698. (Taken from Karapetyan, N. V.; Schubin, V. V.; Strasser, R. J. *Photosynth. Res.* **1999**, *61*, 291−301.)

(26) Small, G. J. *Chem. Phys.* **1995**, *197*, 239−257.

(27) Pullerits, T.; Monshouwer, R.; van Mourik, F.; van Grondelle, R. *Chem. Phys.* **1995**, *194*, 395−407.

(28) Osad'ko, I. S. *Spectroscopy and Excitation Dynamics of Condensed Molecular Systems*; Agranovich, V. M., Hochstrasser, R. M., Eds.; North-Holland Publishing Company: Amsterdam, 1983; Chapter 10.

(29) van Amerongen, H.; Valkunas, L.; van Grondelle, R. *Photosynthetic excitons*; World Scientific Publishing Co. Pte. Ltd.: Singapore, 2000.

(30) Timpmann, K.; Ellervee, A.; Pullerits, T.; Ruus, R.; Sundström, V.; Freiberg, A. *J. Phys. Chem. B* **2001**, *105*, 8436−8444.

(31) Wu, H.-M.; Rätsep, M.; Jankowiak, R.; Cogdell, R. J.; Small, G. J. *J. Phys. Chem. B* **1998**, *102*, 4023−4034.

(32) Wu, H.-M.; Rätsep, M.; Jankowiak, R.; Cogdell, R. J.; Small, G. J. *J. Phys. Chem. B* **1997**, *101*, 7641−7653.

(33) Frese, R.; Palacios, M. A.; Azzizi, A.; van Stokkum, I. H. M.; Kruip, J.; Rögner, M.; Karapetyan, N. V.; Schlodder, E.; van Grondelle, R.; Dekker, J. P. *Biochim. Biophys. Acta* **2002**, *1554*, 180−191.

(34) Birks, J. B. *Rep. Prog. Phys.* **1975**, *38*, 903−974.